Periodica Polytechnica
Civil Engineering

OnlineFirst (2018) paper 11822
https://doi.org/10.3311/PPci.11822

RESEARCH ARTICLE

Study of the Impact of Microstructure and Sorption Properties of the Renovation Plasters on the Wall Drying Rate

Waclaw Brachaczek[1*]

Received 13 December 2017; Revised 27 February 2018; Accepted 20 March 2018

Abstract
The purpose of the study was to determine the relationship between the microstructure and sorption properties of plasters and the drying rate of walls made of sandstone, silicate bricks, ceramic Gothic and Cadinen bricks. The porosity of plasters was 30%, 40% and 50%, and they differed in water sorption. The studies were carried out with one and two layers of plaster. It was demonstrated that the properties of the renovation plasters influence their drying rate. Plasters with a polymodal distribution of pore size and porosity of 50% shortened the wall drying rate, while monomodal distribution and hydrophobic plasters extended the wall drying rate.

Keywords
renovation plasters, walls humidity, microstructure of the renovation plasters, sorption coefficient, porosity

1 Faculty of Materials, Civil and Environmental Engineering
University of Bielsko-Biala
Ul. Willowa 2, 43-300 Bielsko-Biala,
* Corresponding author, email: wbrachaczek@ath.bielsko.pl

1 Introduction

The main factors that lower the durability of walls are salts and moisture. In order to avoid the damage related to salt crystallization, it is necessary to dry the wall and remove the mineral salts. According to construction practice, renovation plasters may be used for this purpose [1]. Due to their properties and microstructure, these plasters are also called wide-pore, salt-absorbing, compressed or lost plasters [2, 3]. The issues of the effectiveness of using renovation plasters as well as the stability of renovation treatments still remain a current topic. In renovating buildings with saline and damp walls, the effects of using renovation plasters are not always satisfactory. This may, on the one hand, be due to workmanship mistakes made during renovation, but also insufficient knowledge about the influence of microstructure of plasters, and their water sorption on the physical phenomenon of drying walls with different properties. [4–6] In the available literature, as well as technical materials supplied by the manufacturers of renovation plasters, information about the recommended thicknesses of each layer, order of their application, and instructions for their use can be found. These parameters are selected based on the measurement of the moisture content of the substrate and the saltiness of the walls. However, the microstructure of the substrate or its water sorption properties are not taken into account. Nonetheless, mismatching the properties of plasters with the properties of substrates may result in a shorter persistence of the renovation treatment, may reduce the stability of the plaster, delay the drying of walls, and accelerate their destruction [7–10].

The current requirements for renovation plasters are included in WTA manual no. 2-9-04 Sanierputzsystemy [11], and standard EN 998-1:2004 [12]. These documents determine the macroscopic properties of components, which are included in the composition of the renovation plaster systems such as porosity, durability, resistance to salt impact etc. They do not, however, include the impact of microstructure of plasters on the wall drying rate, or the reciprocal interaction of plasters on various substrates.

The plasters of the same properties impact the wall drying rate in various ways due to the fact that the walls differ in microstructure and sorption. The premise for writing this article is an attempt to determine the dependence between the sorption and microstructure of renovation plasters on the wall drying rate of various properties.

1.1 Drying of porous materials

According to Lewis [13] the drying of porous materials occurs according to one of two processes: diffusion of moisture from the inside of the solid to the surface and evaporation from the surface of the solid. According to Comings and Sherwood [14] the moisture transport mechanism changes during drying; in the first period the moisture is mainly transported by capillary forces, whereas the diffusion mechanism dominates the second period of drying. According to Kohonen [15], apart from the vapor diffusion (volume diffusion), the water molecules can move over the surface of the pores, or as a result of leaps or unevenness of the fluid layers. This type of transport is called surface diffusion. Drying is nonlinear in nature due to the fact that the physical properties of the dried material change during the drying process, and the physical transition from the liquid phase to the solid phase is nonlinear as well [16]. Pore size distribution, their interconnection, pore mesh geometry, and pore surface properties impact these mechanisms [17, 18]

As the drying progresses, the air enters into larger pores, and the moisture migration proceeds in the same way in the liquid as in the gaseous phase. At the saturation of the liquid phase below a certain critical value X_{Kr}, a thin, stationary sorption film is formed on the surface of the pores. A part of the water is closed by capillary forces in pores of diameter r_m, which depends on the moisture content of the material X. In two-layer systems consisting of a porous substrate covered with plaster layer with varying pore sizes, the moisture transport is completely determined by the capillary pressure difference. Small pores tend to suck water as a result of pressure gradients, while water in large pores evaporates [19, 20].

Liquid pressure p_L [Pa] can be determined as the difference in pressure between the surroundings p_A and the liquid in a single capillary p_C, using the Laplace Eq. (1):

$$p_L = p_A - p_C = -\frac{2 \cdot \gamma \cdot \cos\theta}{r_m} + p_A \quad (1)$$

According to the Eq. (1), the pressure of liquid p_L on a given section depends on: the pore diameter r_m, contact angle θ and surface tension of the liquid γ. If there are some menisci of different diameter in the material, then there will be a pressure gradient between them. According to liquid motion equation, the acceleration vector is directed opposite to the pressure gradient.

Petkovic [10] analyzed the effect of the difference in pore size distribution of porous plaster and substrate on the drying rate and desalination of materials differing in pore size distribution. Based on laboratory tests, it was shown that the process of drying of the samples consisting of the same plaster applied to different materials is different. She stated that this parameter could be impacted by the relationship between the distribution of pore size of the plaster and the substrate. The layers with larger pores, when in hydraulic contact with the layers of smaller diameter, dried first.

Renovation plasters are characterized by a broad pore size distribution. Along with pores of a few micrometers in diameter, they contain wide pores with a diameter of several hundred micrometers. Depending on the characteristics, two basic categories of these plasters are distinguished: salt transporting and accumulating, and hydrophobic ones[10]. In salt transporting and accumulating plasters, there are active capillary pores with a diameter of several to several dozen micrometers, and pores interrupting the liquid flow with a diameter greater than 70 micrometers [21]. In the wide pores, salt accumulating space is created in such a way as to avoid damage due to crystallization. Good efficiency in salt removal and accumulation is achieved by combining transporting and accumulating plasters with hydrophobic into one system. In hydrophobic plasters, the moisture transport in liquid form does not occur. The water, however, is transported outside in the form of vapor, leaving the plaster surface dry and free of blooms. For this reason, it can be stated that the renovation plasters affect the drying rate in a variety of ways.

1.2 Graphical interpretation of material drying

The drying process can be represented graphically with charts showing the changes in moisture content (kg/kg) dependence on the square root of the drying time $\sqrt{t}$, as well as with the drying rate curve obtained by graphical differentiation of the drying curve. In the latter case, the drying rate w is calculated using the Eq. (2):

$$w = -\frac{m_s}{F} \cdot \frac{dX}{dt} \quad (2)$$

where: m_s – mass of the dry material (kg), X – the humidity of the material (moisture content kg per dry mass kg),

F – the dried surface (m^2) based on the geometrical measurement of the wall, t – drying time (s).

An example of a drying curve for porous material is shown in Fig. 1.

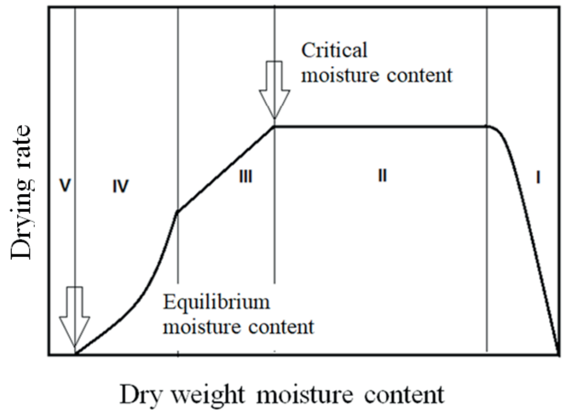

Fig. 1 Drying rate curve

As shown in the chart in Fig. 1, the drying process is divided into the following periods:

- Period I - pre-drying, wherein water evaporates from the surface of the sample and capillary transport of water from the inside of the sample towards its surface is initiated.
- Period II - constant drying rate phase, in which the drying rate is dominated by the flow of moisture (depending on the porous medium) and the evaporation from the surface of the material. Under the defined conditions, the partial pressure of water vapor in the material ambient air pA is fixed and the drying rate is determined by the vapor pressure at the surface of the material, which in the general case depends on the humidity and temperature of the dried material surface. The drying rate in the second period can be represented by the following Eq. (3).

$$-\frac{dX}{dt} = k_g \cdot \left(Y_w - Y\right) \cdot F = const = \beta \qquad (3)$$

where: m_s – mass of the dry material (kg), X – the humidity of the material (moisture content kg per dry mass kg), F – the dried surface (m^2) based on the geometrical measurement of the wall, t – drying time (s), k_g – evaporation rate, β – the drying rate in the second period, Y_w – relative humidity of air over the material, Y – relative air humidity, X – the humidity of the material (moisture content kg per dry mass kg).

For more complex porous structures and a large amount of salt in the wall, the drying rate curve, showing the relationship between $-dX/dt$ of moisture content X may have a more varied shape [4].

- Period III - of decreasing drying rate which starts when the average content in the drying material reaches a critical value X_{kr}. On the surface of the material, dry spots begin to appear and unsaturated drying surface forms. Then, the evaporation of moisture from the increasingly deeper layers of porous material, the movement of water vapor to the surface (inner diffusion) and diffusion in the layer of air flow occur.
- Period IV - following the complete evaporation of moisture from the surface of the material. The determining factor of the drying rate here is the internal movement of moisture. It depends on the moisture concentration gradient between the deeper layers of the material and its surface. Evaporation occurs below the surface of the material in the plane moving more and more into the material as the drying progresses. Water vapor pressure at the surface in this case is lower than the saturation pressure;
- In period V the moisture content in the material reaches equilibrium moisture content and the drying stops.

2 Materials and methods

To determine the type and microstructure of the materials which can be found in building renovation, an analysis of building walls renovated between 2007 and 2013 was conducted. It included 24 buildings erected between XV and XVIII century as well as 54 buildings dated back to XIX century situated in the area of Lower Silesia, Poland. It was determined that in the majority of cases, where the buildings were erected before XIX century, the walls were built of full bricks and sandstone. The most prevailing were hand-formed bricks: Gothic and Cadinen bonded with clay or lime mortar. The Cadinen bricks come from XIX century. The manufacturer was located in Kadyny city in the northern part of Poland by the Vistula Gulf. Due to the exhaustion of the resources of highly plastic clay, the production of Cadinen bricks was ceased at the end of 1970.

Fig. 2 presents the pore size distribution of bricks which come from the selected buildings. The origin of sandstone was difficult to ascertain. It could be assumed that it came from local deposits.

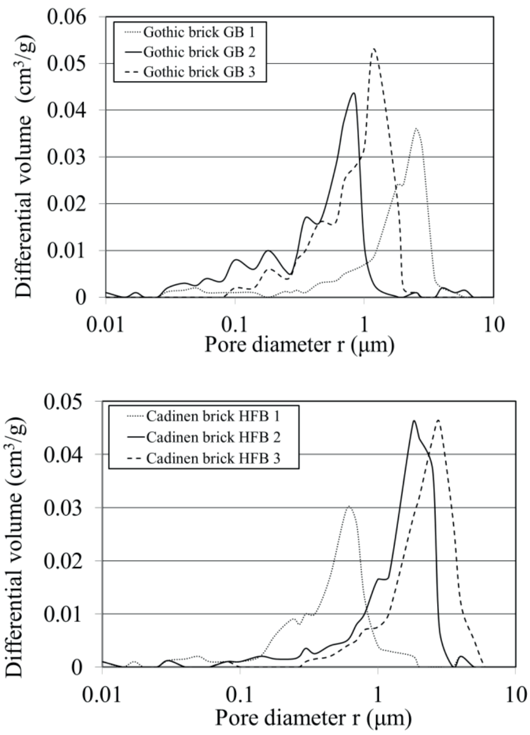

Fig. 2 The distribution of pore sizes in gothic bricks GB (a), Cadinen bricks HFB (b) from different buildings

Following the analysis, the aim of the study was to determine the impact of microstructure of the renovation plasters and their sorption on the drying rate of walls made of Permian sandstone, Slupiec deposit (SS), full bricks: Gothic brick (GB), hand-formed Cadinen brick (HFB), and silicate brick (SB).

The tests were carried out on test walls with the dimensions 740 × 596 × 240 mm. Horizontal joints had a thickness of 12 mm, and vertical ones - 10 mm and were made of M1 class cement and lime mortar (Fig. 4). The changes in moisture content of water-soaked walls covered with one and two plaster layers were studied. Plasters differed in pore size distribution, hydrophobicity of pore surface (hydrophobic and hydrophilic), as well as total porosity of Pc (%) which was 30% and 50% for hydrophilic plasters, and 40% for hydrophobic plasters.

Table 1 The distribution of pore size of materials from which test walls were made

Material	Pc (%)	Pore size distribution (% Pc)					A (kg/(m²·t^0.5))
		<0.01	0.01–0.1	0.1–10	10–100	>100	
GB Gothic brick	31.5	2.8	14.6	61.4	21.2	–	23.4
HFB Cadinen brick	36.3	4.2	15.3	57.3	23.2	–	21.0
SB Silicate brick	17.0	1.5	45.4	52.2	0.9	–	15.2
SS Permian sandstone	14.0	2.3	35.2	62.2	0.3	–	1.3
T I Plaster	32.7	8.4	14.6	64.1	5.2	4.9	3.5
T III Plaster	52.1	0.7	2.1	10.9	31.4	43.4	24.6
HF Plaster	41.6	0.8	1.9	15.7	28.4	48.4	0.9

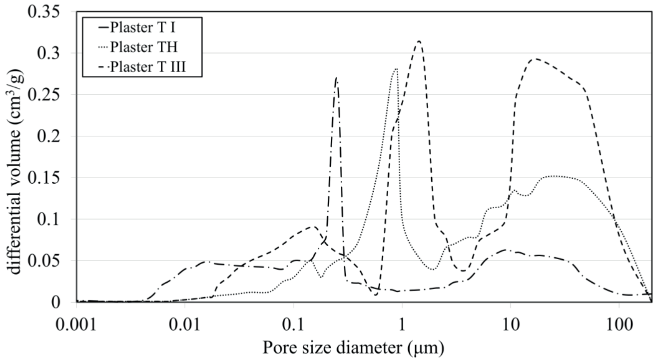

Fig. 3 Differential pore volume distribution according to the pore size diameters for plasters TI, TIII and HF

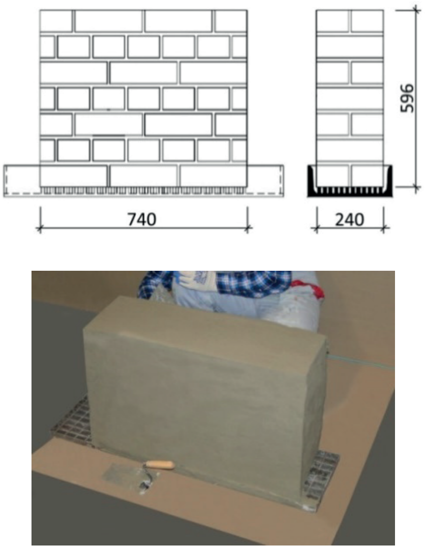

Fig. 4 The dimensions of test walls

For the selected materials, the following physical parameters were marked: values of water sorption coefficients A, porosity P [%]. The obtained values of the parameters are presented in Table 1. The pore size distribution is presented in a graphical form in Fig. 3.

In one-layer plaster systems, the walls were prepared for the study in such a way that when the mortar was hardened, the rendering coat was applied to the lateral surfaces of three walls in a semi-covering method (the degree of coverage was 50%). One layer of suitable plasters was then applied to a thickness of 20 mm.

In systems with two layers of plaster, a non-hydrophobized plaster with a thickness of 20 mm was used as the first layer, while hydrophobized plaster with a thickness of 10 mm as another layer. Once the plaster hardened, test walls were saturated with water by gradually immersing them into a water tank so as to obtain the maximum of moisture content (weight) in the material. To determine the maximum moisture content, parameter w_{max} (kg/kg) can be used. This parameter is calculated based on the Eq. (4).

$$w_{max} = \frac{m_n}{m_s} \tag{4}$$

where: w_{max} – maximum moisture content, parameter w_{max} (kg/kg), m_n – moisture in the state of full saturation (the maximum weight of moisture) (kg), m_s – the mass of a dry sample (kg).

Value w_{max} (kg/kg) for particular bricks was as follows::

Hand-formed Cadinen bricks HFB: w_{max} = 0.133 kg/kg,

Gothic bricks (GB): w_{max} = 0.116 kg/kg,

Sandstone bricks (SS): w_{max} = 0.056 kg/kg,

Silicate bricks: w_{max} = 0.11 kg/kg.

Measurement of the humidity changes in the walls in the drying process was performed using a GE Protimeter Surveymaster hygrometer. The average humidity value obtained from three independent walls was taken as the final result of the measurement. The measurement was carried out at 20°C, and relative air humidity of 55%. Moisture change measurement was carried out until the walls were dried. Walls were considered dry if their humidity was 0.03 kg/kg.

3 Research results and discussion

3.1 Walls with one layer of plaster

Fig. 5 to 8 show drying curves of water-saturated walls made of bricks HFB, GB, SB, and sandstone SS coated with one layer of TI, T III and HF plasters. In each case, the drying curves for plaster walls were compared with raw, not plastered walls.

3.1.1 The impact of microstructure of a plaster on the wall drying rate

The TI plasters, with a porosity of 30%, had little influence on the overall drying time of the walls. Significant predominance of pores with a diameter of 0.3 to 0.5 μm in the total

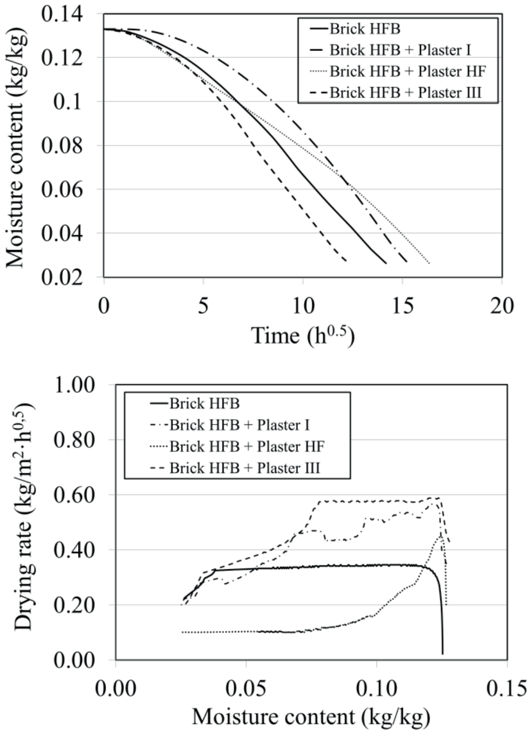

Fig. 5 Drying curves (a) and dependence of drying rate on moisture content (b) determined for raw walls as well as with one layer of TI, T III and HF plasters made of hand-formed Cadinen brick HFB

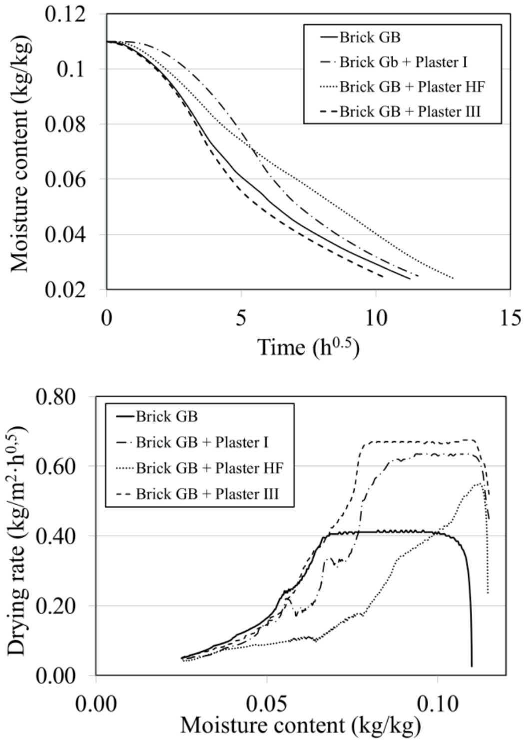

Fig. 6 Drying curves (a) and dependence of drying rate on water content X (b) determined for raw walls as well as with one layer of TI, T III and HF plasters made of Gothic brick GB

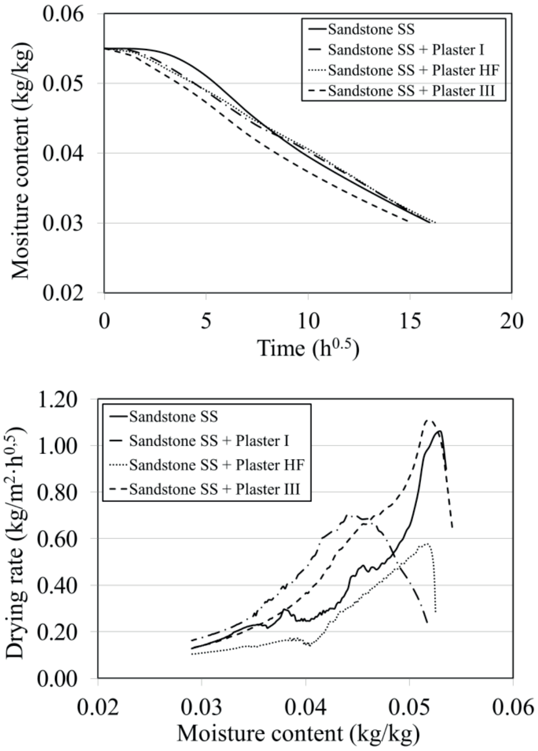

Fig. 7 Drying curves (a) and dependence of drying rate on moisture content (b) determined for raw walls as well as with one layer of TI, T III and HF plasters made of sandstone SS

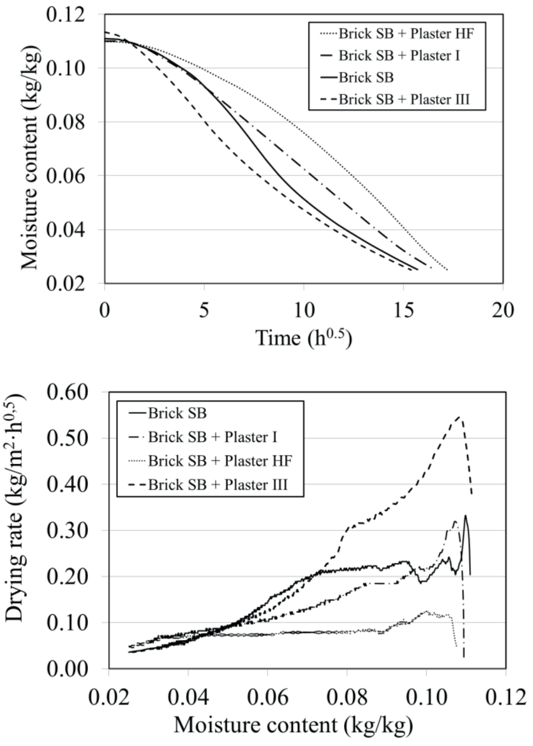

Fig. 8 Drying curves (a) and dependence of drying rate on moisture content (b) determined for raw walls as well as with one layer of TI, T III and HF plasters made of silicate brick SB

pore volume of TI plaster on the one hand, contributed to an increase in drying rate in the second period. On the other hand, drying rate was decreased in the third and fourth periods of drying. The greatest influence of TI plaster on the drying rate in the second period was observed in the case of walls made of HFB and GB bricks, which may be explained by the occurrence of pressure gradient resulting from the capillary effect of the plaster on the substrate. The drop of drying rate in the third and fourth periods, as compared to non-plastered walls, can be explained by a small volume percentage of pores with a diameter greater than 100 µm, which hinders the diffusion of water vapor towards the wall surface. As a consequence, the walls covered with TI plaster dried slower than the non-plastered walls.

Walls covered with T III plasters with a porosity of 50% and polymodal size distribution dried faster than non-plastered walls. The greatest impact on the increase in the drying rate in the second period was observed for walls made of bricks HFB and GB. The increase in the drying rate at this period can be linked to the high volume of capillary-active pores with a diameter of 0.5 to 70 µm, which is approx. 40%. In accordance with the Eq. (1), in the material for which $\cos\theta > 0$, the liquid pressure decreases with decreasing pore diameter. It can therefore be concluded that in a specific small segment of the material, liquid fills all the capillaries with radii smaller than rm. As a result of the pressure gradient presence, pores with a smaller diameter tend to suck water from pores with a larger diameter [19].

Shortening of the drying time is also be impacted by the transport of moisture through the diffusion of water vapor, which is fostered by a significant volume of air pores in the total porosity. This is evidenced by the higher values of humidity X_{kr}, which, when exceeded, marks the beginning of the third drying period.

In the case of SS and SB, higher drying rates were also observed in the second period as compared to non-plastered walls. However, due to the large number of fine pores determined in SS and SB, the pressure gradient associated with capillary action was lower than for HFB or GB. The second drying period occurred in a narrow range of changes in humidity X and was related to the drying of the plaster layer itself rather than the entire wall.

In the case of walls covered with HF hydrophobic plaster, no second drying period was observed, which means that the drying was related to moisture transport by volume diffusion through the plaster layer from increasingly deeper layers of the wall. The absence of the second period in this case is related to the hydrophobic nature of the pore surface. The hydrophobic plaster lengthened the total wall drying time. The reason for this mechanism is low plaster water sorption coefficient, which was obtained by hydrophobizing the surface of the pores with a polymethylsiloxane-based admixture. In a hydrophobic material for which $\cos\theta < 0$, the liquid pressure, according to Eq. (1), decreases with the increase of the capillary radius. In this case, the liquid fills all the capillaries with radii of more than *rm*. For HF plasters, irrespective of pore size distribution, drying occurs only through the diffusion of water vapor [20] [22].

3.1.2 The impact of water sorption coefficient of the wall on the drying rate

In the case of GB, HFB bricks and T III plaster, the values of A coefficients were similar: 23.4 for GB, 21.0 for HFB and 24.6 kg/($m^2 \cdot t^{0.5}$) for T III as shown in Table 1. For the sandstone and silicate bricks, the lower values of these coefficients were determined, as follows: 1.3 kg/($m^2 \cdot t^{0.5}$) for SS and 15.2 kg/($m^2 \cdot t^{0.5}$)for SB. Lower values of A coefficient for SS and SB were also associated with a significant shortening of the second drying period, which caused the drying in this case to occur mainly through water vapor diffusion. Thus, the effect of T III plaster on the total drying time was lower for walls made of sandstone or silicate bricks than for brick walls with higher coefficients of water sorption A. Differences in the total drying rate of walls made of various materials are presented in Fig. 10.

3.2 Walls with two layers of plaster

Drying curves of water-saturated walls made of bricks HFB, GB, SB, and sandstone SS covered with two layers of plaster are presented in Fig. 9. T III plaster was selected as the first layer because it had the greatest impact on the wall drying rate. HF plaster was used as the second layer. This arrangement should prevent the moisture in the liquid phase from penetrating into the outer surface of the plaster.

When analyzing the diagram of the walls drying rate with two layers, where one is hydrophobic (Fig. 9), the following conclusions can be stated:

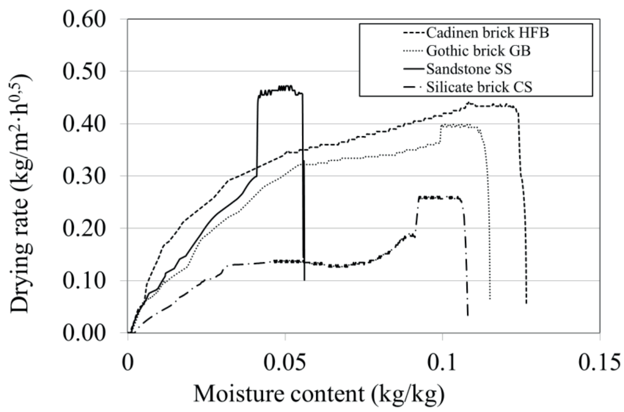

Fig. 9 Dependence of the drying rate on the moisture content in the material, determined for walls made of GB, HFB, SS sandstone and SB silicate bricks covered with two layers of plasters: T III and HF

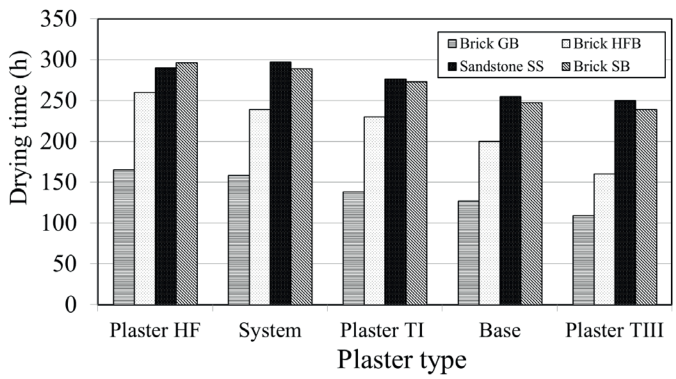

Fig. 10 Comparison of wall drying time to an moisture content of 0.03 kg/kg of walls made of various materials: covered with two plasters T III and HF, with walls covered with one layer of plasters: HF, TI, III and not plastered base

- The curves clearly show drying periods connected with the flow of moisture in the liquid phase as well as with water vapor diffusion. It may be assumed that these changes are influenced by low resistance of water vapor diffusion through the hydrophobic plaster layer. Moisture in the liquid phase reaches the interface of T III/FH plasters, where it evaporates.

- It has been found that in each case the humidity range of the material for the second drying period has decreased. The values of critical moisture X_{kr} were higher for walls with two layers than in the case of one layer of T III plaster.

- The walls made of SB silicate bricks dried in the second period at a lower rate than the walls made of HFB or GB bricks. In the case of walls made of sandstone, characterized by the lowest absorbability, only a short increase in the drying rate in the second period was observed, followed by a significant decrease in the rate in the third and fourth periods.

Fig. 9 shows the total drying time of the walls to moisture content of 0.03 kg/kg with single layers of plaster as well as the system consisting of T III plaster and HF plaster.

The water sorption coefficient of the material from which the walls A were built also influenced the drying rate. Walls made of HFB and GB bricks dried faster than the walls made of SS or SB with lower water sorption coefficient A.

4 Conclusions

The research presented in this paper shows that the walls of historical buildings show a great diversity in respect of microstructure or its water sorption properties.

The dependence of the relationship between plaster/substrate pore size distribution has an impact on the wall drying rate. Adopting total porosity values for renovation plasters as a basic selection criterion in the renovation of damp and salty walls may be insufficient. Plasters should be selected in such a way as to assure a pressure gradient caused by the capillary action of the plaster against the substrate.

The results show that the T III plaster with porosity of 50% and the polymodal distribution of pore size is a good solution as the first plastering layer, directly adjacent to the dried wall.

Analyzing the impact of the sorption coefficient on the drying rate, it can be concluded that regardless of the type of material from which the walls were made, the walls which were the slowest to dry, were coated with plasters of low A coefficients.

The renovation of highly damp and salty walls should be performed in two steps with the application of two types of plaster. The first layer should be made of plasters with over 50% porosity and polymodal pore size distribution. The latter layer - the final one - should be hydrophobic.

The works should be performed in the summer periods at low air humidity.

Significant air pore predominance - capillarily inactive in the first layer of plaster - causes the salts to largely crystallize inside the porous plaster.

At high wall saltiness, after initial wall drying, these plasters can be removed and replaced with new plasters, or after cleaning the surface, they can be covered with hydrophobic one.

References

[1] Meier, H. G. "*Sanierputze: ein wichtiger Bestandteil der Bauwerksinstandsetzung*". Expert, 2002.

[2] Pavlikova, M., Pavlik, Z., Keppert, M., Cerny, R. "Salt transport and storage parameters of renovation plasters and their possible effects on restored buildings′ walls". *Construction and Building Materials*, 25(3), pp. 1205–1212. 2011. https://doi.org/10.1016/j.conbuildmat.2010.09.034

[3] Dettmering, T., Kollmann, H. "*Putze in Bausanierung und Denkmalpflege*". Beuth Verlag, Berlin, 2012.

[4] Groot, C., Van Hees, R. P. J., Wijffels, T. "Selection of plasters and renders for salt laden masonry ubstrates". *Construction and Building Materials*, 23(5), pp. 1743–1750. 2009. https://doi.org/10.1016/j.conbuildmat.2008.09.013

[5] Van Hees, R. P. J., Naldini, S., Rodrigues, J. D. "Plasters and renders for salt laden substrates". *Construction and Building Materials*, 23(5), pp. 1714–1718. 2009. https://doi.org/10.1016/j.conbuildmat.2008.09.009

[6] Lubelli, B., Van Hees, R. P. J., Groot, C.W. P. "Investigation on the behaviour of a restoration plaster applied on heavy salt loaded masonry". *Construction and Building Materials*, 20(9), pp. 691–699. 2006. https://doi.org/10.1016/j.conbuildmat.2005.02.010

[7] Collepardi, M. "Degradation and restoration of masonry walls of historical buildings". *Materials and structures*, 23(2)pp. 81–102. 1990. https://doi.org/10.1007/BF02472568

[8] Collepardi, M. "Thaumasite formation and deterioration in historic buildings". *Cement & Concrete Composites*, 21(2), pp. 147–154, 1999. https://doi.org/10.1016/S0958-9465(98)00044-4

[9] Shahidzadeh-Bonn, N., Rafai, S., Bonn, D., Wegdam, G. "Salt crystallization during evaporation: Impact of interfacial properties". *Langmuir*, 24(16), pp. 8599–8605. 2008. https://doi.org/10.1021/la8005629

[10] Petkovic, J., Huinink, H. P., Pel, L., Kopinga, K., Van Hees, R. P. J. "Salt transport in plaster/substrate layers". *Materials and Structures*, 40(5), pp. 475–490. 2007. https://doi.org/10.1617/s11527-006-9151-7

[11] WTA Merkblatt 2-9-04/D:2005-10. "*Sanierputzsysteme*". Technische Regel, DIN Deutsches Institut für Normung e. V., 2005.

[12] PN-EN 998-1:2004 Wymagania dotyczące zapraw do murów Część 1: Zaprawa tynkarska (The requirements regarding the mortars - Part 1 : Plastering Mortars).

[13] Lewis, W. K. "The rate of drying of solid materials". *The Industrial and Engineering Chemistry*, 13(5), pp. 427–432. 1921. https://doi.org/10.1021/ie50137a021

[14] Comings, E. W., Sherwood, T. K. "The drying of solids. VII. Moisture movement by capillarity in drying granular materials". *Industrial and Engineering Chemistry*, 26(10), pp. 1096–1098. 1934. https://doi.org/10.1021/ie50298a017

[15] Kohonen. R. "*A method to analyze the transient hygrothermal behavior of building materials and components*". Technical Research Centre of Finland, Publication 21, pp. 33–39. 1984.

[16] Kowalski, S. J. "Toward a thermodynamics and mechanics of drying processes". *Chemical Engineering Science*, 55(7), pp. 1289–1304. 2000. https://doi.org/10.1016/S0009-2509(99)00400-5

[17] L. Bagel, L., Zivica, V. "Relationship between pore structure and permeability of hardened cement mortars: On the choice of effective pore structure parameter". *Cement and Concrete Research*, 27(8), pp. 1225–1235. 1997. https://doi.org/10.1016/S0008-8846(97)00111-7

[18] Kunito, T., Honda, A.,Mashima, M., Hamasato, S. "A study on the relationship between pore structure and coefficient of permeability of soil stabilized with cement". *MRS Proceedings*, 137, p. 457. 1989. https://doi.org/10.1557/PROC-137-457

[19] Hall, C., Hoff, W. D. "*Water transportin brick, stone and concrete*". CRC Press, 2011. https://doi.org/10.1201/b12840

[20] Hall, C., Hoff, W.D. "Rising damp: capillary rise dynamics in walls". *Proceedings of the Royal Society – Mathematical Physical and Engineering Sciences*, 463(2084), pp. 1871-1884. 2007. https://doi.org/10.1098/rspa.2007.1855

[21] Dullien, F.A.L. "*Porousmedia: fluid transport and pore structure*", Academic press, 1992.

[22] Alsabry, A. "Dynamika podciągania kapilarnego w murach budowlanych. (The dynamics in capillaryrise in building walls)", Przegląd budowlany. 9, pp. 46–48. 2010. http://www.przegladbudowlany.pl/2010/09/2010-09-PB-46-48_Alsabry.pdf